CrystEngComm

Accepted Manuscript

ROYAL SOCIETY OF CHEMISTRY

www.rsc.org/crystengcomm

Journal Name

RSCPublishing

ARTICLE

Supramolecular Assemblies of Ru(II) Organometallic Half-Sandwich Complexes

Cite this: DOI: 10.1039/x0xx00000x

Bao Cheng[a], Alireza Azhdari Tehrani[b], Mao-Lin Hu[a]*, Ali Morsali[b]*

Received 00th January 2012,
Accepted 00th January 2012

DOI: 10.1039/x0xx00000x

www.rsc.org/

A series of new Ru(II) half-sandwich complexes with the general formula of [(arene)Ru(L)Cl_2], where L is a monodentate amine ligand and arene is a *p*-cymene or benzene ring were synthesized, characterized and their supramolecular structures were analyzed. The crystal packing of these compounds was studied with the aid of geometrical analysis, Hirshfeld surface analysis and theoretical calculations. Our study reveals the importance of three common hydrogen bonding motifs as the primary factor controlling the supramolecular architecture of these series of complexes. Furthermore, the role of amine ligand substituent could be different, depending on the type of interactions that occurs between functional groups. Interestingly, homomeric self-complementary intermolecular interactions are formed, when the ancillary ligand contains benzyl cyanide or alkyl 4-aminobenzoate. These non-conventional interactions could be promising for the design of organometallic supramolecular arrays.

Introduction

In recent years, crystal engineering of metal-containing compounds has attracted increasing interests due to their potential applications in diverse areas.[1] Since many of the bulk properties of molecular materials are dictated by the manner in which the molecules (building blocks) are assembled in the solid state, it is clear that the ability to control this ordering would afford control over these properties. Despite recent advances,[2] crystal engineering of inorganic and organometallic compounds is still in its infancy due to the complexities in predicting the structural outcome of the supramolecular architecture. Among these, organometallic crystal engineering is very similar to organic crystal engineering.[3] This is because the metal centers in organometallic compounds are mostly buried by the organic outer portion of the molecules and the metal atoms are not directly involved in intermolecular interactions. Thus, many factors that play important roles in controlling the architecture of self-assembled organometallic species are the same as those known in organic crystal engineering.[3a,c] Accordingly, functional groups on the ligands and the non-covalent interactions that occur between them are crucial in determining the crystal structures of organometallic compounds. Considering these point, many attempts have been aimed at understanding the supramolecular chemistry of the sandwich and half-sandwich organometallic complexes.[4] Among the half-sandwich complexes, arene ruthenium complexes of the three-legged piano-stool type are recently considered as building blocks for the construction of desired architectures due to their versatile applications in different fields, from catalysis to medicine.[5] In this regard, Bacchi, Pelegatti and their co-workers studied the effects of different monodentate amines on the construction of supramolecular wheel-and-axle metal-organic (WAAMO) systems based on [(*p*-cymene)Ru(κN-H_2N-COOH)], where the terminal wheels are half sandwich units, [(*p*-cymene)$RuCl_2$], and the axles are based on the dimeric carboxylic O-H···O synthon.[6]

In this paper we report an extension of these studies aimed at understanding the supramolecular features of [(arene)Ru(L)Cl_2], where L is a monodentate amine ligand and arene is a *p*-cymene or benzene ring, complexes. Eight new half-sandwich Ru(II) complexes [(η^6-*p*-cymene)Ru(4-aminobenzonitrile)Cl_2] (**1**), [(η^6-*p*-cymene)Ru(4-aminobenzylcyanide)Cl_2] (**2**), [(η^6-*p*-cymene)Ru(4-aminophenyl acetic acid)Cl_2] (**3**), [(η^6-*p*-cymene)Ru(methyl 4-aminobenzoate)Cl_2] (**4**), [(η^6-*p*-cymene)Ru(ethyl 4-aminobenzoate)Cl_2] (**5**), [(η^6-*p*-cymene)Ru(butyl 4-aminobenzoate)Cl_2] (**6**), [(η^6-C_6H_6)Ru(ethyl 4-aminobenzoate)Cl_2] (**7**), [(η^6-C_6H_6)Ru(butyl 4-aminobenzoate)Cl_2] (**8**) have been prepared, characterized, and their crystal structures determined. Complexes synthesized here are schematically shown in Scheme 1, where X and Y represent the arene and amine ligand's substituents, respectively. The crystal packing of these compounds, as well as the packing of related compounds retrieved from Cambridge Structural Database,[7] was studied with the aid of geometrical analysis, Hirshfeld surface analysis,[8] and theoretical calculations. The study reveals that in most cases the crystal packing of these complexes is firstly driven by one of the three extended hydrogen bonding motifs between half-sandwich units which is followed by the formation of weak intermolecular interactions between functional groups of the ancillary ligand (L).

Results and Discussion

Synthesis

Complexes **1**-**6** were prepared from the reaction of [(η^6-*p*-cymene)$RuCl_2]_2$ with a 2-fold excess of corresponding *para*-substituted aniline ligands, in dry methanol under an inert atmosphere of nitrogen. Also, the reaction of (η^6-C_6H_6)$RuCl_2$ with ethyl 4-aminobenzoate and butyl 4-aminobenzoate, under the same reaction condition, gave complexes **7** and **8**, respectively. These

complexes were characterized by NMR and IR spectroscopy. The X-ray quality crystals of **1**,**2**,**4**,**5** and **6** were grown by slow evaporation technique, using methanol or methanol/dichloromethane mixture, as stated in experimental section, while the single crystals of **3**,**7** and **8** were obtained by slow diffusion of diethyl ether into a MeOH:DCM mixture. The crystallographic data for complexes **1**-**8** are listed in Table 1. Selected bond length and angles are summarized in Table S1.

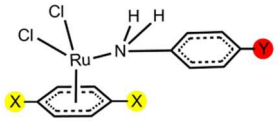

Complex	X	Y
1	Me, i-Pr	CN
2	Me, i-Pr	CH_2CN
3	Me, i-Pr	CH_2COOH
4	Me, i-Pr	COOMe
5	Me, i-Pr	COOEt
6	Me, i-Pr	COOBu
7	H, H	COOEt
8	H, H	COOBu

Scheme 1. Representation of the synthesized [(arene)Ru(*para*-substituted amine)Cl_2] complexes.

Structural analyses of complexes [(η^6-*p*-cymene)Ru(4-aminobenzonitrile)Cl_2] (1), [(η^6-*p*-cymene)Ru(4-aminobenzylcyanide)Cl_2] (2)

X-ray crystallography analyses reveal that both complexes crystallize in monoclinic $P2_1/c$ space group. ORTEP diagrams of **1**-**8** drawn with 30% probability have been shown in Figure S1 (Supporting Information). In these complexes, the coordination geometry around the Ru(II) atom can be described as pseudo-octahedral, with three sites occupied by the η^6-*p*-cymene ligand and the remaining three by the two chloride and the *para*-substituted aniline ligands, with bond lengths and angles of Ru-N(2)=2.18(1) Å, N(2)-Ru-Cl(1)=80.3(2)° and N(2)-Ru-Cl(2)=82.7(2)° for **1** and Ru-N(2)=2.172(4) Å, N(2)-Ru-Cl(1)=82.0(1)° and N(2)-Ru-Cl(2)=80.5(1)° for **2** (Table S1). The ruthenium atom is situated 1.655 and 1.662 Å from the centroid of the *para*-cymene ring in **1** and **2**, respectively.

In the crystal packing of **1**, centrosymmetric dimeric units of [(η^6-*p*-cymene)Ru(4-aminobenzonitrile)Cl_2] are formed by two $_{cym}$C-H···Cl interactions between the arene CHs and the metal bound chlorides of pairs of complexes. Adjacent dimeric units are further linked to each other by C-H···N_{CN}, N-H···N_{CN}, in *ab*-plane, N-H···Cl and weak π_{cym}-π_{phen} stacking (ring centroid to ring centroid distance=4.190 Å), along the *a*-axis, forming the 3D crystal packing (Figure 1a, Table S2). Parameters for selected hydrogen bonding interactions are collected in Table S2. In the case of **2**, similarly the centrosymmetric dimeric units of [(η^6-*p*-cymene)Ru(4-aminobenzylcyanide)Cl_2] are formed via $_{cym}$C-H···Cl hydrogen bonds of unequal length. These dimers are further linked to adjacent dimers via $R_2^2(6)$ C-H···C_{CN} intermolecular interactions formed between benzyl cyanide moieties of neighboring molecules (Figure 1b and Table S2), thus leading to the construction of wheel-and-axle supramolecular assembly.[6b-d] A Cambridge Structural Database (with the help of ConQuest version 1.16)[7] search was undertaken to find the frequency of occurrence of C-H···C_{CN} interaction. The results show that this type of intermolecular interaction has occurred in almost seventeen percent of the CSD hits. The percentage was calculated as the number of observed C-H···C_{CN} hits (2276 hits) divided by the total number of potential hits (13219 hits) in the database (Figure S10). Also a CSD search on $R_2^2(6)$ C-H···C_{CN} interaction returned 142 hits (no disorder and error free). Filtering the results, by excluding the hits in which MeCN presents as a solvent of crystallization, gave 47 hits with C-H···C_{CN} distance ranging from 2.57 to 2.89 Å. Therefore, this non-conventional cyclic supramolecular synthon could be a potential supramolecular glue to assemble organic, inorganic and organometallic building blocks.

Furthermore, the intermolecular interactions in the crystal structure of **1** and **2** are quantified via Hirshfeld surface analysis[8] using Crystal Explorer 3.0.[9] Hirshfeld surface analysis is a novel tool for the visualization and understanding of intermolecular interactions. A histogram of percentage contributions of different intermolecular interactions is shown in Figure 6a. All the C-H, O-H and N-H distances were normalized to neutron lengths. The histogram indicates that, in both cases, the H···H interactions are indeed the dominating ones (the highest contribution to the Hirshfeld surface) and from **1** to **2**, by replacing 4-aminobenzonitrile with 4-aminobenzylcyanide, the contribution of the C···H interaction increases (from 10.7% to 13.6%), while the contribution of C···C decreases (from 4.7% to 1.5%).

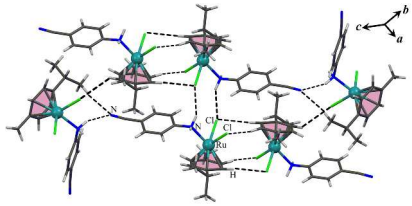

(a)

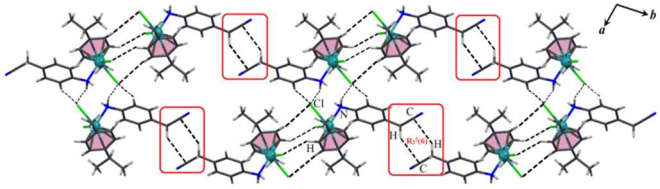

(b)

Figure 1. A side view representation of [(η^6-*p*-cymene)Ru(4-aminobenzonitrile)Cl_2], **1,** showing the association of the half-sandwich units through N-H…Cl and $_{cym}$-H…Cl hydrogen bonds along the *a*-axis and C-H···N_{CN}, N-H···N_{CN} to generation of 3D crystal packing (a). A side view representation of [(η^6-*p*-cymene)Ru(4-aminobenzylcyanide)Cl_2], **2**, in *ab*-plane, showing the association of dimers via $R_2^2(6)$ C-H···C_{CN} intermolecular interactions formed between benzyl cyanide moieties of neighboring molecules (b).

Structural analysis of complex [(η^6-*p*-cymene)Ru(4-aminophenyl acetic acid)Cl_2] (3)

Complex **3** crystallizes in monoclinic $P2_1/n$ space group. The pseudo-octahedral coordination sphere around the Ru(II) atom is

Table 1. Structural data and refinement parameters for compounds **1-8**.

	1	**2**	**3**	**4**	**5**	**6**	**7**	**8**
formula	$C_{17}H_{20}Cl_2N_2Ru$	$C_{18}H_{22}Cl_2N_2Ru$	$C_{18}H_{23}Cl_2NO_2Ru$	$C_{18}H_{23}Cl_2NO_2Ru$	$C_{19}H_{25}Cl_2NO_2Ru$	$C_{21}H_{29}Cl_2NO_2Ru$	$C_{15}H_{17}Cl_2NO_2Ru$	$C_{17}H_{21}Cl_2NO_2Ru$
fw	424.32	438.35	457.34	457.34	471.37	499.42	415.27	443.32
λ/Å	0.71073	0.71073	0.71073	0.71073	0.71073	0.71073	0.71073	0.71073
T/K	298	298	298	298	298	298	298	298
crystal system	Monoclinic	Monoclinic	Monoclinic	Triclinic	Triclinic	Triclinic	Monoclinic	Triclinic
space group	$P2_1/c$	$P2_1/c$	$P2_1/n$	$P\bar{1}$	$P\bar{1}$	$P\bar{1}$	$P2_1/c$	$P\bar{1}$
a/Å	9.0285(15)	10.1443(17)	9.240(2)	7.8773(16)	9.7344(14)	7.8252(17)	13.3810(14)	6.6232(8)
b/Å	12.877(2)	18.539(3)	21.764(5)	9.0893(19)	13.158(2)	9.227(2)	8.9330(9)	8.5047(10)
c/Å	17.446(3)	11.6609(15)	9.576(2)	14.820(3)	16.451(2)	17.196(4)	13.2711(13)	16.752(2)
α/°	90.0	90.0	90.0	87.187(4)	97.681(3)	77.288(4)	90.0	101.870(2)
β/°	119.823(7)	122.580(10)	102.591(4)	83.837(3)	92.007(3)	80.060(4)	95.693(2)	96.297(3)
γ/°	90.0	90.0	90.0	70.569(3)	106.116(3)	69.450(4)	90.0	98.447(2)
V/Å^3	1759.7(5)	1847.9(5)	1879.4(7)	994.8(4)	2000.3(5)	1127.9(4)	1578.5(3)	903.83(19)
D_{calc}/Mg.m^{-3}	1.602	1.576	1.616	1.527	1.565	1.471	1.747	1.629
Z	4	4	4	2	4	2	4	2
μ (mm^{-1})	1.192	1.138	1.128	1.066	1.063	0.947	1.334	1.170
F(000)	856	888	928	624	960	512	832	448
2θ (°)	50.04	56.32	50.66	50.00	50.20	50.18	50.08	50.20
R (int)	0.0472	0.0279	0.0415	0.0186	0.0294	0.0248	0.0631	0.0505
GOOF	1.410	1.334	1.363	1.427	1.297	1.286	1.441	1.334
R_1[a](I>2σ(I))	0.0912	0.0537	0.0827	0.0544	0.0998	0.0686	0.1411	0.1364
wR_2[b](I>2σ(I))	0.1606	0.1500	0.1395	0.1615	0.2314	0.1596	0.2543	0.2899
CCDC No.	996321	996322	996323	996324	996325	996326	996327	996328

[a] $R_1 = \Sigma||F_o| - |F_c||/\Sigma|F_o|$. [b] $wR_2 = [\Sigma(w(F_o^2 - F_c^2)^2)/\Sigma w(F_o^2)2]^{1/2}$.

completed with the η^6-coordinated-*p*-cymene ring (ring-centroid to Ru distance=1.660 Å), two chloride and the NH_2 group of 4-aminophenyl acetic acid (Ru-N(1)=2.168 (6) Å, N(1)-Ru-Cl(1)=85.9(2)° and N(1)-Ru-Cl(2)=79.2(2) °), (Table S1).

In the crystal structure of **3**, the N-H···Cl interactions involve one of the NH hydrogen atoms of the 4-aminophenyl acetic acid to the metal bound chloride forming dimeric unit in an inverted fashion. The carboxylic group donates a hydrogen bond to chloride, O(1)-H(1)···Cl(1), while accepting hydrogen bond from the remaining NH hydrogen atom, N(1)-H(1B)···O(2), for the generation of hydrogen bonded chain along the *a*-axis (Figure 2).

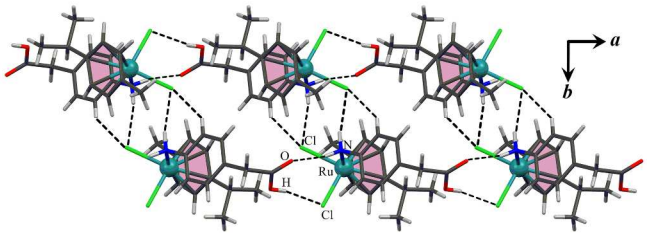

Figure 2. A side view representation of [(η^6-*p*-cymene)Ru(4-aminophenyl acetic acid)Cl_2], **3**, in *ab*-plane, showing the association of the adjacent molecules through O-H···Cl and N-H···O hydrogen bonds to generation of linear chain. These chains are further linked to each other by N-H…Cl and C_{phen}-H…Cl interactions.

The crystal packing analysis of [(η^6-*p*-cymene)Ru(4-aminobenzoic acid)Cl_2] reveals formation of WAAMO system assembled by the $R_2^2(8)$ cyclic hydrogen-bonded carboxylic homodimer synthon.[6b] The only difference between [(η^6-*p*-cymene)Ru(4-aminobenzoic acid)Cl_2] and **3** is the presence of an additional methylene group in the amine ligand of the latter complex. This leads to the disruption of the expected carboxylic dimer synthon and hence preventing the formation of WAAMO pattern.

The contribution percentages of different interactions to the Hirshfeld surface areas are shown in Figure 6a. It should be noted that the similarity in the percentage of O···H interactions to the Hirshfeld surface area in both complexes is ascribed to different intermolecular interactions, namely N-H···O for **3** and O-H···O for [(η^6-*p*-cymene)Ru(4-aminobenzoic acid)Cl_2].

Structural analyses of complexes [(η^6-*p*-cymene)Ru(methyl 4-aminobenzoate)Cl_2] (4), [(η^6-*p*-cymene)Ru(ethyl 4-aminobenzoate)Cl_2] (5), [(η^6-*p*-cymene)Ru(butyl 4-aminobenzoate)Cl_2] (6)

4, **5** and **6** crystallize in the centrosymmetric triclinic space group $P\bar{1}$. The asymmetric units of **4** and **6** consist of one crystallographically independent molecule, Z′=1, whereas the asymmetric unit of **5** contains two half-sandwich Ru(II) complexes, Z′=2. The coordination sphere of the Ru(II) center is completed by an η^6 π-bounded *p*-cymene ring, two chloride ions and the nitrogen atom of the alkyl 4-aminobenzoate ligands. The Ru-N(1) bond distances are 2.184(5) Å for **4**, 2.171(9) Å for **5** and 2.18(1) Å for **6**, Table S1. The distances between ruthenium and the centroid of the *p*-cymene ring are 1.652 Å, 1.653 and 1.663 Å, 1.656 Å for **4**, **5**, **6**, respectively. In the crystal packing of **4** and **6**, each NH_2 group is coordinated to the metal center that bridges two half-sandwich complexes, in *a*-direction, which are cooperated with $_{cym}$C-H···Cl hydrogen bonds between the arene CHs and the metal bound chloride to generate an infinite double stranded chain (motif (A) in scheme 2a). Common extended hydrogen bonding motifs observed in Ru(II) half-sandwich complexes are shown in Scheme 2. It is apparent that a good match between hydrogen bond donors and acceptors, both in number and spatial arrangement, is necessary for

the formation of these hydrogen bonding motifs. The double stranded chain is then linked to adjacent chains via C-H···O hydrogen bonds forming $R_2^2(10)$, for **4**, and $R_2^2(14)$, for **6**, ring motifs between the alkyl ester groups (Figure 3a,b). In case of **6**, the C-H···O interactions forming the $R_2^2(14)$ synthon occurs slightly above the sum of the Van der Waals radii of two atoms[10] (Table S2).

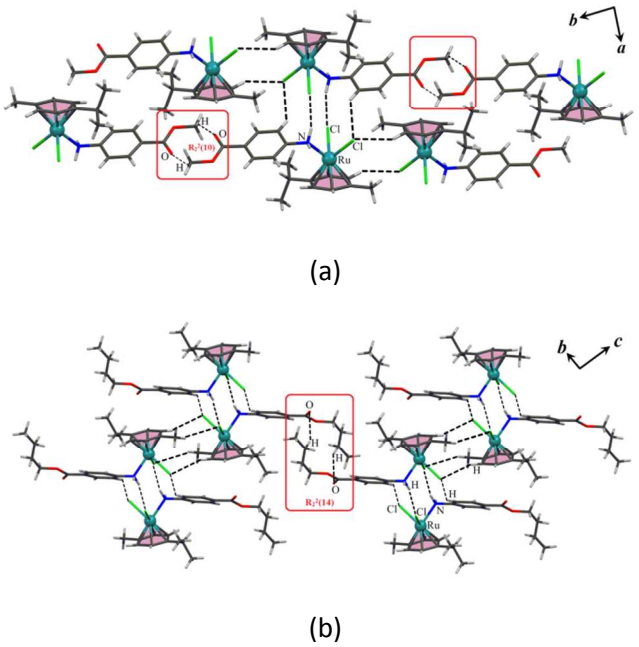

Figure 3. Representations of [(η^6-*p*-cymene)Ru(methyl 4-aminobenzoate)Cl_2], **4**, in *ab*-plane, (a) and [(η^6-*p*-cymene)Ru(butyl 4-aminobenzoate)Cl_2], **6**, in *bc*-plane, (b), Showing the association of half-sandwich units through extended hydrogen bonding motif (A) and generation of weak self-complementary $R_2^2(10)$, for **4**, and $R_2^2(14)$, for **6**, synthons between the alkyl ester groups

In **5**, the half-sandwich Ru(II) independent molecules are held together, in a way almost identical to motif (A), by N-H···Cl and C-H···Cl hydrogen bonds. The only difference between the hydrogen bonding motif in **5** and those observed in **4**, **6** is rooted in different behavior of NH_2 groups in bridging adjacent molecules. Thus, while the NH_2 function of half-sandwich complex containing Ru(1), donates two hydrogen bonds to two chloride atoms on two neighboring molecules, the NH_2 group of another independent molecule containing Ru(2), involved in only one N-H···Cl close contact. The overall supramolecular structure results from the linkage of neighboring chains via C-H···O_{CO} hydrogen bonds in *bc*-plane (Figure 4a,b and Table S2).

Table 2 provides a summary of the crystal packing features of the series of [(arene)Ru(*para*-substituted amine)Cl_2], that have been reported so far. From this Table, it can be concluded that motif (A) is the most common hydrogen bonding motif in these classes of complexes. Interestingly, all the Ru(II) half-sandwich complexes that show motif (A), Scheme 2a, were crystallize in the triclinic space group $P\bar{1}$.

Another interesting feature, in the crystal structures of **4** and **6,** is that there is a tendency to form weak self-complementary intermolecular interactions between the alkyl ester groups which act as the supramolecular axle for the construction of the WAAMO system. A simple survey, in the CSD, shows that this non-conventional $R_2^2(10)$ (2415 hits) and $R_2^2(14)$ (394 hits) hydrogen bonding synthons between alkyl ester groups are not rare, but have received less attention due to their inherent weakness. Hirshfeld surface analysis also reveals that, upon the extension of the alkyl chain length, the probability of H···H interaction increases, while that of O···H and Cl···H decreases (Figure 6b). It was thought of interest to further investigate the binding energies of cyclic hydrogen-bonded synthons in these series of complexes, by using theoretical methods. The binding energies obtained from DFT on two relative fragments from **2**, **4**, **6**, and for the sake of comparison studies have also been carried out on [(η^6-*p*-cymene)Ru(4-amino benzoic acid)Cl_2],[6b] [(η^6-*p*-cymene)Ru(4-aminobenzamide)Cl_2],[6d] complexes (Figure S9, supporting information). This provides us an opportunity to evaluate the complexes involving cyclic supramolecular synthon, forming the axle of the WAAMO system. The outcomes obtained from DFT methods are listed in Table 2. The resulting binding energy is in agreement with the classification of hydrogen bonding types.[11] It is to be noted that in the case of **6**, the binding energy does not represent the energy of C-H···O hydrogen bonding interactions individually, but it reflects an overall binding energy from a combination of C-H···O and several H···H interactions. As expected, the binding energies of the complexes studied here, **2**, **4** and **6**, are in the range of weak hydrogen bonding energies. Thus, the results revealed that, along with the formation of extended hydrogen bonding between half-sandwich units, a wide range of intermolecular interactions, from weak to strong, can play the role of supramolecular axle in the construction of WAAMO pattern.

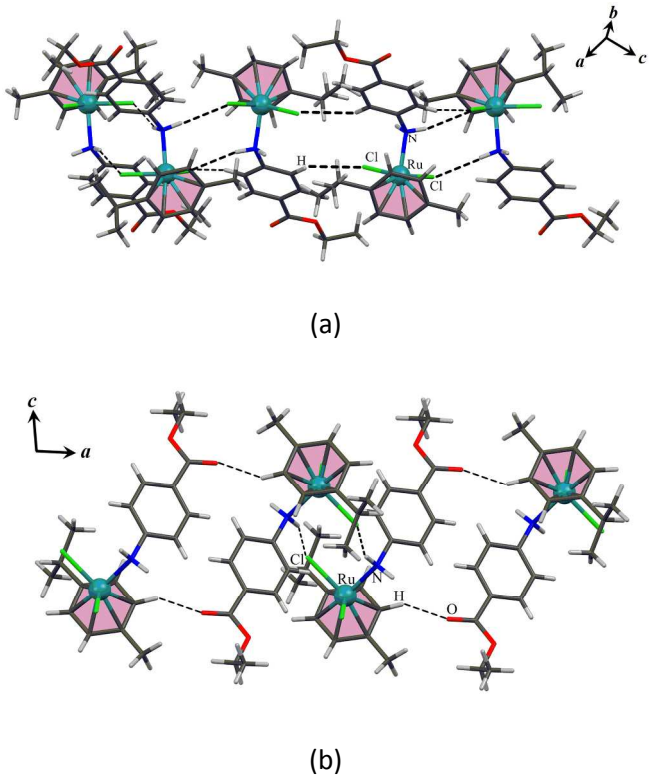

Figure 4. A side view representation of [(η^6-*p*-cymene)Ru(ethyl 4-aminobenzoate)Cl_2], **5**, showing the association of adjacent molecules through N-H…Cl and C_{phen}-H…Cl hydrogen bonds, similar to motif (A) (a). Presence of C_{cym}-H···O hydrogen bonds, between adjacent dimers, in *ac*-plane (b).

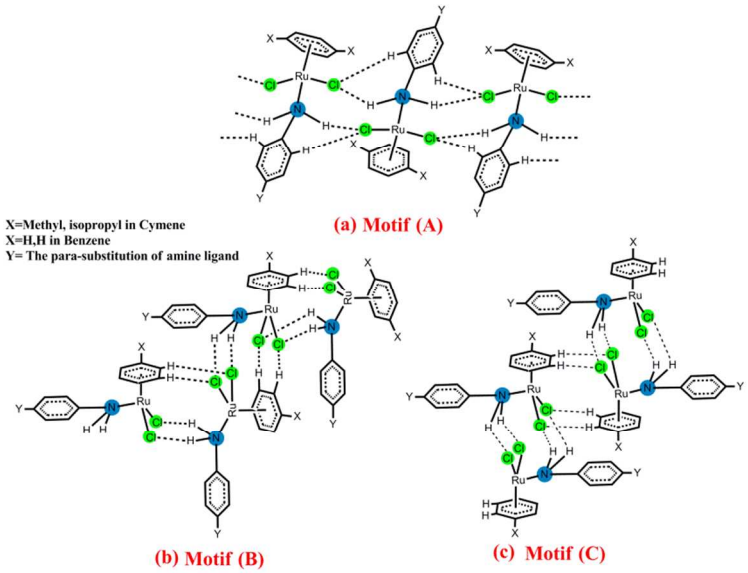

Scheme 2. Common extended hydrogen bonding motifs observed in Ru(II) half-sandwich complexes with the general formula of [(arene)Ru(*para*-substituted amine)Cl_2].

Structural analyses of complexes [(η^6-C_6H_6)Ru(ethyl 4-aminobenzoate)Cl_2] (7) and [(η^6-C_6H_6)Ru(butyl 4-aminobenzoate)Cl_2] (8)

Crystallographic analyses reveal that **7** crystallizes in monoclinic $P2_1/n$ space group, while **8** crystallizes in the triclinic space group $P\bar{1}$. In these compounds, the coordination geometry around the Ru(II) ion is similar to that observed in **1**-**6**, i.e., pseudo-octahedral with three sites occupied by the η^6-benzene ligand and the three remaining positions by the two chloride ions and the nitrogen atom of the alkyl 4-aminobenzoate ligand. The Ru-N bond distances are 2.16(1), 2.18(1) Å, for **7** and **8**, respectively (Table S1). The Ru atom is located at 1.641 Å, for **7**, and 1.643 Å, for **8**, from the centroid of the benzene ring.

In the crystal packing of **7**, dimeric units are formed by a pair of $_{Benz}$C-H···Cl and N-H···Cl hydrogen bonding interactions between the half-sandwich units while they are almost perpendicularly oriented to one another (motif (B) in Scheme 2b and Figure 5a). Thus, a linear hydrogen-bonded chain is formed from these dimeric units in the *b*-direction. This motif has been previously observed in two different non-solvated polymorphs of [(η^6-*p*-cymene)Ru(4-aminobenzamide)Cl_2].[6d] These chains are further linked to one another, in *ab*-plane, by $_{Benz}$C-H···O_{CO} hydrogen bonds (Figure 5a and Table S2).

In the case of **8**, inverted dimeric units of **8** are stabilized by a pair of $_{Benz}$C-H···Cl interactions between the arene CHs and the metal bound chlorides of pairs of complexes. These dimeric units are connected to each other by N-H···Cl interactions to form a hydrogen bonded network along the *b*-axis (Figure 5b and Table S2). According to Table 2, the supramolecular hydrogen bonding motif (B) is also observed in the case of [(η^6-*p*-cymene)Ru(4-methylaniline)Cl_2][12] and one of the polymorphs of [(indane)Ru(4-aminobenzoic acid)Cl_2][6b] (Table 2). It should be noted that the oxygen atoms of esteric group are not involved in any close contact. The crystal packing analyses of **5**, **6**, **7** and **8** reveal that the less-hindered nature of the benzene ring, compared to the cymene, allows

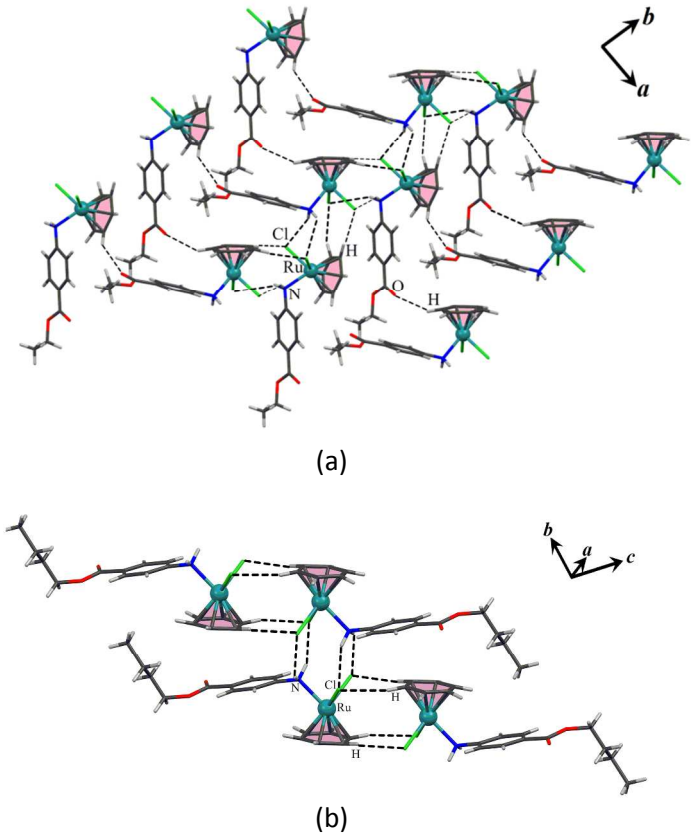

Figure 5. A side view representation of [(η^6-C_6H_6)Ru(ethyl 4-aminobenzoate)Cl_2], **7**, in *ab*-plane, showing the formation of a linear hydrogen-bonded chain via C-H···Cl and N-H···Cl interactions along the *b*-axis. These chains are further linked to each other, in *ab*-plane, by $_{Benz}$C-H···O_{CO} hydrogen bonds. (a) Formation of extended hydrogen bonding motif (C) in [(η^6-C_6H_6)Ru(butyl 4-aminobenzoate)Cl_2], **8**

Table 2. Crystal packing features of the series of [(arene)Ru(*para*-substituted amine)Cl_2]

Compound	Type of amine ligand (L)	Hydrogen bonding motif	Space group	Inverted Piano-Stool	WAAMO pattern	Calculated energy of dimeric synthon (kJ/mol)	Refcode
[(Cymene)Ru(L)Cl_2]	4-fluoroaniline	-	$P2_1/n$	Yes	-		QAHYUV
[(Cymene)Ru(L)Cl_2]	4-chloroanilne	-	$P2_1/n$	Yes	-		DEFRIQ
[(Cymene)Ru(L)Cl_2]	4-aminobenzoic acid	Motif (A)	$P\bar{1}$	Yes	Yes	-96.84	PAMDUE
[(Cymene)Ru(L)Cl_2]. C_2H_5OH	4-aminocynnamic acid	-	$F2dd$	-	-		PAMFEQ
[(Cymene)Ru(L)Cl_2]. H_2O	4-aminocynnamic acid	-	$P2_1/n$	-	-		PAMFAM
[(Cymene)Ru(L)Cl_2]. C_3H_6O	4-aminocynnamic acid	Motif (A)	$P\bar{1}$	Yes	Yes		PAMFIU
[(Cymene)Ru(L)Cl_2]	4-amino-3-hydroxybenzoic acid	-	$P1$	-	Yes		HELGAI
[(Cymene)Ru(L)Cl_2]	3-amino-4-hydroxybenzoic acid	-	$P2_1/c$	-	Yes		HELGEM
[(Cymene)Ru(L)Cl_2]	1,3-diisopropylbenzene	-	Cc	Yes	-		ROMKEJ
[(Cymene)Ru(L)Cl_2]	1,3-diisopropylbenzene	-	$C2/c$	-	-		ROMKEJ01
[(Cymene)Ru(L)Cl_2]	4-methylaniline	Motif (C)	$P2_1/n$	Yes	-		TAJFUF
[(Cymene)Ru(L)Cl_2]	4-aminobenzamide	Motif (B)	$C2/c$	-	Yes	-52.19	PIYTOI
[(Cymene)Ru(L)Cl_2]	4-aminobenzamide	Motif (B)	$P1$	-	Yes		PIYTOI01
[(Cymene)Ru(L)Cl_2]. MeOH	4-aminobenzamide	Motif (A)	$P\bar{1}$	Yes	-		SIMPIP
[(Cymene)Ru(L)Cl_2]. H_2O	4-aminobenzanilide	-	$P\bar{1}$	Yes	-		SIMPUB
[(Cymene)Ru(L)Cl_2]. C_2H_5OH	4-aminobenzanilide	Motif (A)	$P\bar{1}$	Yes	-		SIMPOV
[(Indane)Ru(L)Cl_2]	4-aminobenzoic acid	Motif (A)	$P\bar{1}$	Yes	Yes		PAMFOA
[(Indane)Ru(L)Cl_2]	4-aminobenzoic acid	Motif (C)	$P\bar{1}$	Yes	Yes		PAMFOA01
[(benzene)Ru(L)Cl_2]. H_2O	4-aminobenzoic acid	Motif (A)	$P\bar{1}$	-	-		PAMGAN
[(Cymene)Ru(L)Cl_2]	4-aminobenzonitrile	-	$P2_1/c$	Yes	-		This work
[(Cymene)Ru(L)Cl_2]	4-aminobenzyl cyanide	-	$P2_1/c$	Yes	Yes	-17.37	This work
[(Cymene)Ru(L)Cl_2]	4-aminophenylacetic acid	-	$P2_1/n$	-	-		This work
[(Cymene)Ru(L)Cl_2]	methyl 4-aminobenzoate	Motif (A)	$P\bar{1}$	Yes	Yes	-17.54	This work
[(Cymene)Ru(L)Cl_2]	ethyl 4-aminobenzoate	Pseudo-Motif (A)	$P\bar{1}$	Yes	-		This work
[(Cymene)Ru(L)Cl_2]	butyl 4-aminobenzoate	Motif (A)	$P\bar{1}$	Yes	Yes	-47.49	This work
[(benzene)Ru(L)Cl_2]	ethyl 4-aminobenzoate	Motif (B)	$P2_1/c$	-	-		This work
[(benzene)Ru(L)Cl_2]	butyl 4-aminobenzoate	Motif (C)	$P\bar{1}$	Yes	-		This work

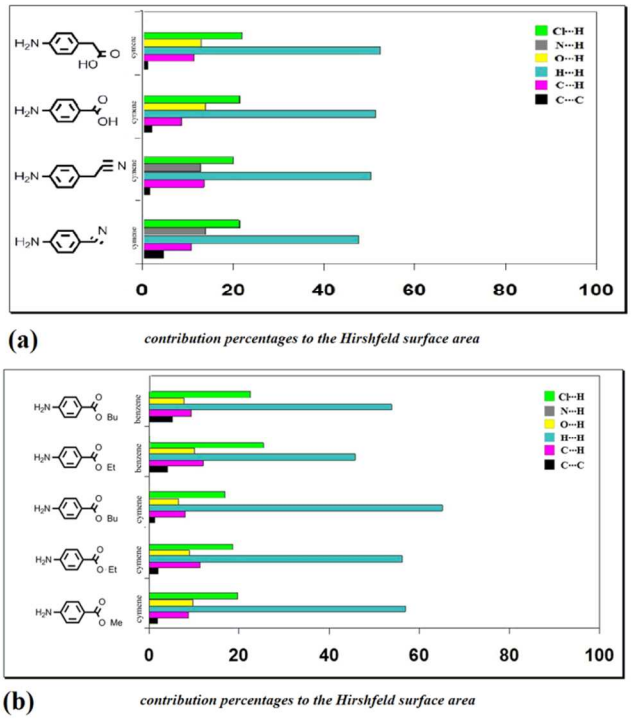

Figure 6. Relative contributions of various intermolecular contacts to the Hirshfeld surface area in complexes **1-3** and [(η^6-*p*-cymene)Ru(4-aminobenzoic acid)Cl_2][6b] (a) and **4-8** (b).

a close approach of neighboring complexes necessary for the formation of an intermolecular π–π stacking interactions, centroid to centroid distances are 4.155 and 3.899Å for **7** and **8**, respectively. Interestingly, the emergence of the π–π stacking interactions suppressed the formation of self-complementary hydrogen bonding synthons, between alkyl ester groups. Thus the results suggest that competition between weak intermolecular interactions may determine the overall supramolecular structure.

A comparison between significant intermolecular interactions controlling the packing of **7** and **8** revealed similar results to those mentioned in the case of **4**, **5** and **6**. Thus, the contribution of H···H interactions increases and the O···H or Cl···H interactions decreases on going from **7** to **8**. The histogram chart also indicates that the replacement of *p*-cymene by the less hindered benzene ring increases the probability of π···π stacking and C-H···π interactions, while that of H···H decreases (Figure 6b).

Conclusions

Eight Ru(II) half-sandwich complexes, [(arene)Ru(L)Cl_2], where L is a monodentate amine ligand and arene is a *p*-cymene or benzene ring, synthesized, characterized and their supramolecular structures were analyzed. A general survey on the reported half-sandwich Ru(II) complexes, with the general formula of [(arene)Ru(*para*-substituted amine)Cl_2], and those presented here indicates three common hydrogen bonding motifs between half-sandwich units. In these motifs, there is a good balance between the number of hydrogen bond donor (two N-H groups) and hydrogen bond acceptor (two metal bound chloride). Among these, motif (A) is the most common in this class of compounds. It is to be noted that motif (C) contains inverted piano-stool dimer, which is itself stabilized by weak C-H···Cl interactions. From Table 2, it is found that motif (A) and (C) take place in the centrosymmetric space groups, while motif (B) may appear in a non-centrosymmetric space group, such as *P*1. The results also suggest that in the presence of an extra hydrogen bond donor, such as the cases of solvent-containing species, the inverted piano-stool motif, and therefore motif (A) and (C), is lost in favor of stronger hydrogen bond interactions. In such half-sandwich complexes of the three-legged piano stool type, the functional group on the amine ligand is an important factor determining the final supramolecular architecture. Functional groups such as carboxylic acid and amide are usually known to form robust self-complementary supramolecular synthons that may be used for the design of extended supramolecular assemblies based on hydrogen bonding. In the absence of such functional groups, weak intermolecular interactions have been identified to play key roles in directing the crystal packing. As examples of this, it is shown here that homomeric self-complementary intermolecular interactions are formed, when the ancillary ligand contains benzyl cyanide or alkyl 4-aminobenzoate. These non-conventional interactions could prove to be a good supramolecular synthon for the design of supramolecular architectures. Thus, a wide range of intermolecular interactions, from weak to strong, can play the role of supramolecular axle in the construction of the WAAMO pattern. Accordingly and based on the DFT calculations, it is explicit that the energy of cyclic hydrogen-bonded synthons vary within a range of −17.37 to −96.84 kJ·mol^{-1}. Noticeably, the tendency of these organometallic entities to form solvates decreased by decreasing the strength of hydrogen bonding in the axle of WAAMO pattern. Thus, our attempts to prepare solvates from **1-8** were unsuccessful. The results of this study should provide insight into the construction of supramolecular assemblies based on organometallic building blocks.

Experimental section

Apparatus and reagents

In addition to [Ru(η^6-*p*-cymene)Cl_2]$_2$ and [(η^6-C_6H_6)$RuCl_2$]$_2$ were synthesized, all other chemicals and solvents were purchased from Aldrich Chemical Company or other commercial vendors and used as received. ^{1}H and ^{13}C NMR spectra were recorded on a Bruker AVANCE-500 spectrometer using tetramethylsilane (TMS) as an internal standard and DMSO-d_6 as the solvent at room temperature. IR spectra were recorded on a Perkin-Elmer Model 1725X spectrophotometer (KBr pellets). Melting points were obtained by a WRS-2A digital melting point apparatus (Shanghai ShenGuang Instrument).

Single-Crystal Diffraction Studies.

Crystallographic measurements of compounds **1-8** were made using a Bruker APEX area-detector diffractometer. The intensity data were collected using graphite monochromated Mo–Kα radiation (λ=0.71073 Å) at 298 K. Cell parameters were retrieved using SMART software and refined with SAINT on all observed reflections.[13] Data reduction was performed with the SAINT software. Absorption corrections were applied with the program SADABS.[14] The structures were solved by direct methods with SHELXS-97.[15] The refinement and all further calculations were carried out with SHELXL-97.[15] It is to be noted that, ethyl, isopropyl

and butyl groups, in **4-6**, and the carbon atoms of benzene rings, in **7**and 8, have a high thermal parameter due to data collection in room temperature. We tried refining these atoms in two positions with reduced occupancy but while this model converged satisfactorily, there was no decrease in *R* value and therefore we consider that our original refinement is the best that can be achieved and should be reported.

General Procedure.

All reactions, if not otherwise stated, were carried out under an inert atmosphere of dry nitrogen, using standard Schlenk techniques. Solvents were dried prior to use and stored over activated molecular sieves. The starting compound, $[Ru(\eta^6\text{-}p\text{-cymene})Cl_2]_2$ and $[(\eta^6\text{-}C_6H_6)RuCl_2]_2$ were synthesized as described in the literature.[16] The complexes were synthesized using a common procedure: (i) the starting ruthenium dimer was dissolved in 10mL of anhydrous methanol and the red solution degassed with nitrogen for 10 min; (ii) under a flow of nitrogen, two equivalents of the ligand was added and the brown-red mixture stirred for 6-8 h at 60℃. The volume of the reaction mixture was slowly condensed to ca. 2mL on a rotary evaporator; (iii) the solution was cooled, the brown-red suspension that resulted was filtered and the solid washed with ether and dried at the vacuum line. The brown-red solid may be crystallized from methanol and ether.[6b]

Computational Details.

DFT calculations were performed using the ORCA quantum chemistry suite.[17] The BLYP exchange–correlation functional[18] with the recent D3 empirical dispersion correction[19] (BLYP-D3) was used in all calculations. The basis set superposition error (BSSE) is not taken into consideration because small BSSE effects are assumed to be absorbed by the D3 empirical potential.[20] The selected two fragments, were cut out directly from the CIF data without optimization. All C-H, O-H and N-H distances were normalized to neutron values and thus these values were retained for the energy calculations. Large atom basis sets TZP are used to ascribe all the atoms here. A frozen core approximation was used to treat the core electrons. Scalar relativistic effects were taken into account by using the zeroth-order regular approximation (ZORA).[21]

Acknowledgements

The authors thank Tarbiat Modares University for all the supports. The work was supported by the National Natural Science Foundation of China (no. 21371137).

Notes and references

[a] College of Chemistry and Materials Engineering, Wenzhou University, Wenzhou, China
[b] Department of Chemistry, Faculty of Sciences, Tarbiat Modares University, P.O. Box 14115-175, Tehran, Iran
Electronic Supplementary Information (ESI) available: [X-ray crystallographic files (CIF), Experimental details, ORTEP diagrams for compounds **1-8**, selected fragments for hydrogen bonding interaction energy analysis, selected bond distances and angles and hydrogen bond geometries for compounds **1-8**]. See DOI: 10.1039/b000000x/

References

(1) (a) S. G. Telfer, R. Kuroda, *Coord. Chem. Rev*., 2003, 242, 33–46 (b) B. Moulton, M. J. Zaworotko, *Chem. Rev*., 2001, 101,1629–1658 (c) E. R. T. Tiekink, J. Zukerman-Schpector, *CrystEngComm*, 2009, 11, 1176−1186 (d) A. K. Hall, J. M. Harrowfield, A. Morsali, A. A. Soudi, A. Yanovsky, *CrystEngComm*, 2000, 2, 82-85 (e) D. Braga, *J. Chem. Soc*., *Dalton Trans*., 2000, 3705–3713 (f) L. Brammer, *Chem. Soc. Rev.*, 2004, 33, 476–489. (g) M. Hong, *Cryst. Growth Des.*, 2007, 7, 10–14.
(2) (a) J. Reedijk, *Chem. Soc. Rev*., 2013, 42, 1776-1783. (b) R. Chakrabarty, P. S. Mukherjee, P. J. Stang, *Chem. Rev*. 2011, 111, 6810–6918. (c) E.C. Constable, *Chem. Soc. Rev*., 2007, 36, 246–253 (d) L. F. Lindoy, K-M. Park, S. S. Lee, *Chem. Soc. Rev*., 2013, 42, 1713 (e) K. Akhbari, A. Morsali, *Coord. Chem. Rev.*, 2010, 254, 1977-2006 (f) M-L. Hu, A. Morsali, L. Aboutorabi, *Coord. Chem. Rev*., 2011, 255, 2821-2859 (g) H. R. Khavasi, A. Azhdari Tehrani, *Inorg. Chem.*, 2013, 52, 2891–2905.
(3) (a) D. Braga, F. Grepioni, G. R. Desiraju, *Chem. Rev.* 1998, 98, 1375-1405 (b) D. Braga, L. Maini, F. Grepioni, *Angew. Chem. Int. Ed.* 1998, 37, 2240-2242 (c) D. Braga, F. Grepioni, *Coord. Chem. Rev.*, 1999, 183, 19-41 (d) D. Braga, F. Grepioni, *J. Chem. Soc*., *Dalton Trans*., 1999, 1–8 (e) L. Brammer, J.C. Mareque Rivas, R. Atencio, S. Fang, F. C. Pigge, *J. Chem. Soc., Dalton Trans.,* 2000, 3855-3867 (f) Y. Kim, J. G. Verkade, *Inorg. Chem.* 2003, *42*, 4262-4264. (g) R. Atencio, L. Brammer, S. Fang, F. C. Pigge, *New J. Chem*., 1999, 23, 461-463.
(4) for example see: (a) D. Braga, L. Maini, M. Polito, E. Tagliavini, F. Grepioni, *Coord. Chem. Rev.*, 2003, 246, 53–71 (b) D. Braga, M. Polito, F. Grepioni, *Cryst. Growth Des.*, 2004, 4, 769-774 (c) D. Braga, S. d'Agostino, F. Grepioni, *Organometallics,* 2012, 31, 1688−1695
(5) (a) P. Kumar, R. Kumar Gupta, D. S. Pandey, *Chem. Soc. Rev.,* 2014, 43, 707-733 (b) C. M. Clavel, E. Păunescu, P. Nowak-Sliwinska, P. J. Dyson, *Chem. Sci*., 2014, 5, 1097–1101 (c) T. Sumiyoshi, T. B. Gunnoe, J. L. Petersen, P. D. Boyle, *Inorg. Chim. Acta*, 2008, 361, 3254–3262 (d) S. E. Dann, S. E. Durran, M. R. J. Elsegood, M. B. Smith, P. M. Staniland, S. Talib, S. H. Dale, *J. Organomet. Chem*., 2006, 691, 4829–4842 (e) A. A. Nazarov, C. G. Hartinger, P. J. Dyson, *J. Organomet. Chem*., 2014, 751, 251–260 (f) A.K. Singh, D. S. Pandey, Q. Xu, P. Braunstein, *Coord. Chem. Rev.*, 2013, http://dx.doi.org/10.1016/j.ccr.2013.09.009 (g) S. T. N. Freeman, F. R. Lemke, L. Brammer, *Organometallics,* 2002, *21,* 2030-2032.
(6) (a) A. Bacchi, M. Carcelli, Pelagatti, P. *Cryst. Rev*., 2012, 18, 253-279 (b) A. Bacchi, G. Cantoni, M. Granelli, S. Mazza, P. Pelagatti, G. Rispoli, *Cryst. Growth Des.*, 2011, 11, 5039–5047 (c) A. Bacchi, G. Cantoni, F. Mezzadri, P. Pelagatti, *Cryst. Growth Des.*, 2012, 12, 4240−4247 (d) A. Bacchi, G. Cantoni, D. Crocco, M. Granelli, P. Pagano, P. Pelagatti, *CrystEngComm*, 2014, 16, 1001-1009 (e) A. Bacchi, G. Cantoni, M. R. Chierotti, A. Girlando, R. Gobetto, J. Lapadula, P. Pelagatti, A. Sironi, M. Zecchini, *CrystEngComm*, 2011, 13, 4365-4375.
(7) Cambridge Structural Database, version 5.35 (Last update may 2014); CCDC: Cambridge, U.K., November 2013.
(8) (a) J. J. McKinnon, M. A. Spackman, A. S. Mitchell, *Acta Crystallogr*., 2004, B60, 627-668 (b) M. A. Spackman, J. J. McKinnon, *CrystEngComm*, 2002, 4, 378-392.
(9) S. K. Wolff, D. J. Grimwood, J. J. McKinnon, M. J. Turner, D. Jayatilaka, M. A. Spackman, *CrystalExplorer 3.0*, University of Western Australia, Perth, Australia, 2012.
(10) A. Bondi, *J. Phys. Chem*. 1964, 68, 441−451.
(11) (a) G. R. Desiraju, *Angew. Chem. Int. Ed.* 2011, 50, 52–59 (b) G. R. Desiraju, *Chem. Commun*., 2005, 2995–3001
(12) M.J. Begley, S. Harrison, A.H. Wright, *Acta Crystallogr*., 1991, C47, 318-320.
(13) Bruker (2007). SMART, SAINT & SADABS. Bruker AXS Inc., Madison, Wisconsin, USA
(14) Bruker (2007). SMART, SAINT & SADABS. Bruker AXS Inc., Madison, Wisconsin, USA
(15) G. M. Sheldrick, *Acta Crystallogr*. 2008, A64, 112
(16) M.A. Bennett, A.K. Smith, *J. Chem. Soc*., *Dalton Trans*. 1974, 233–241.
(17) F. Neese, U. Becker, D. Ganyushin, D. G. Liakos, S. Kossmann, T. Petrenko, C. Riplinger, F. Wennmohs, ORCA, 2.7.0; University of Bonn: Bonn, 2009.
(18) (a) A. D. Becke, *Phys. Rev*., 1988, 38, 3098 (b) C. Lee, W. Yang and R. G. Parr, *Phys. Rev. B: Condens. Matter Mater. Phys*., 1988, 37, 785.
(19) S. Grimme, J. Antony, S. Ehrlich and H. Krieg, *J. Chem. Phys*., 2010, 132, 154104.
(20) C. Fonseca Guerra, H. Zijlstra, G. Paragi and M. Bickelhaupt, *Chem.–Eur. J.*, 2011, 17, 12612.

(21) (a) E. van Lenthe, E. J. Baerends, J. G. Snijders, *J. Chem. Phys.*1993, 99, 4597−4610 (b) E. van Lenthe, E. J. Baerends, J. G. Snijders, *J. Chem. Phys.* 1994, 101, 9783−9792 (c) E. van Lenthe, R. van Leeuwen, E. J. Baerends, J. G. Snijders, *Int. J. Quantum Chem.* 1996, *57*, 281−293

Graphical Abstract

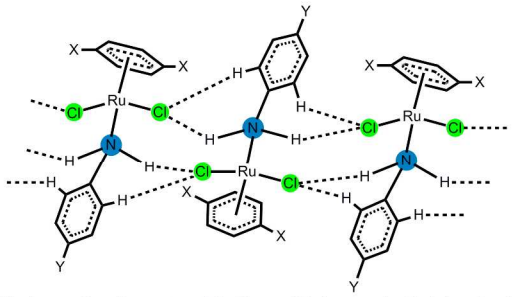

Extended hydrogen bonding network in [(arene)Ru(para-substituted amine ligand)Cl_2]